Quantifying Ultrasonic Deformation of Cell Membranes with Ultra-High-Speed Imaging

A. Marek[1], A. De Grazia[1], X. Régal[1], D. Carugo[1] and F. Pierron[1]

Faculty of Engineering and Physical Sciences

University of Southampton, Southampton, UK

ABSTRACT

We present a new method for controllable loading of cell models in an ultrasonic (20 kHz) regime. The protocol is based on the inertial-based ultrasonic shaking test and allows to deform cells in the range of few mm/m to help understand potential consequences of repeated loading characteristic to ultrasonic cutting.

Keywords: Ultra-high speed imaging, ultrasound, GUVs, IBUS, mechanobiology

INTRODUCTION

Ultrasonically-powered cutting tools are a promising alternative for cutting hard tissues with higher precision and lower damage compared to the currently employed tools. During a surgical procedure a fresh scalpel causes cell deaths in a nearby region called a 'zone of cell death' (several hundreds of micrometers wide) slowing down the healing process [1]. Ultrasonic cutting tools have a potential to reduce/control the width of the zone of cell death. However, the interaction between the ultrasonic loading and cell apoptosis is still not well established.

The oscillating cutting blade interacts with the cutting sites and produces repeated deformation that travels through extracellular matrix (ECM) in form of mechanical waves. As the ECM deforms, so do the cells attached to it which in turns can lead to activation of molecular pathways leading to apoptosis, or potentially healing as used in low intensity pulsed ultrasound (LIPUS) treatments [2-4]. Due to high frequency nature of the loading it is very difficult to reproduce *in vitro* the dynamic loading that is relatable to what the cells experience *in vivo*.

The most common experimental techniques to study biological effects of ultrasonic loading on cellular entities are cavitation tests (often leading to sonoporation) [5, 6] and direct exposure to acoustic waves in liquid media [7, 8]. The former represents much more violent stimulus, not necessarily applicable to the cutting scenario, while the latter makes oversimplified assumptions regarding acoustic conditions (pressure) such as lack of reflections, no formation of standing waves etc. and does not measure the deformation of cells directly.

In this contribution we propose a test based on inertial-based ultrasonic shaking test (IBUS) [9] in which cells are attached to a substrate deforming with ultrasonic frequency, thus transferring the loading onto them. For this task we use a cell membrane model, giant unilamellar vesicles (GUVs) that consist of lipid bilayer enclosing aqueous. The substrate is made out of clear PMMA and allows to image the deforming cells in real time using ultra-high speed camera (Shimadzu HPV-X).

We demonstrate that the attached GUVs deform with the same frequency and strain amplitude as the substrate calibrated using the IBUS test and so the test offers an interesting platform to study biological effects of attached cells under known amplitude of ultrasonic deformation. In future, this platform could be used to study fatigue of cell membrane, as well as biological responses of living cells to a known history of mechanical/thermal stimuli.

METHODS

The protocol consists of two steps: preparing and calibrating the substrate according to the IBUS test and then imaging deformation of attached GUVs under a bright field microscope setup.

In the first step, clear PMMA coupons (55 × 20 × 3 mm) were laser-cut from a 3 mm thick sheet (Perspex) and tested following the IBUS procedure. The coupon's length was selected such that its first longitudinal mode corresponds to 20 kHz excitation. One face of the coupon was covered with white acrylic paint and printed with a regular pattern of grid (0.82 mm pitch) to measure full-field displacements using the grid method (**Fig. 1**) [10], while the other side was covered with black acrylic paint to facilitate temperature measurements. The coupon was glued to a sonotrode (SinapTec NexTgen) that excites one of the edges at 20 kHz. The sonotrode was programmed to oscillate at a known fraction of its maximal amplitude and the corresponding deformation was measured using an ultra-high speed camera (Shimadzu HPV-X) recording at 500 kfps. From these measurements it was possible to calibrate amplitude of longitudinal strain at each of the sections of the specimen with the sonotrode power, avoiding the need for direct measurements in subsequent tests.

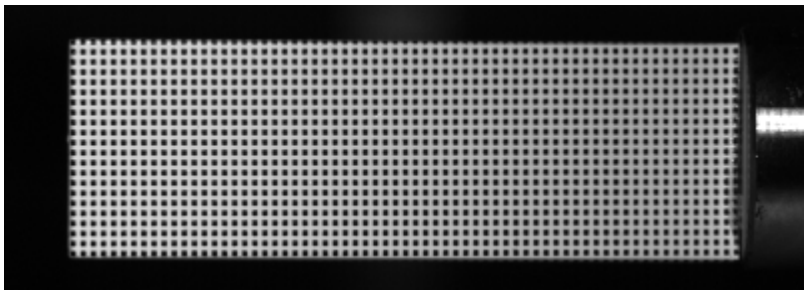

Fig. 1 An image of the PMMA coupon covered with regular grid for measuring displacements using the grid method.

The second step consists of preparing GUVs and functionalizing the PMMA coupons such that they can be used to transfer the ultrasonic loading onto the vesicles. First, an O-ring was attached at the middle of the coupon using a silicone gel so that the stiffness (and thus the resonance response) of the coupon is not altered (**Fig. 2**(a)). The O-ring serves as a well to contain liquid solutions needed to keep and attach GUVs on the substrate. To bio-functionalize the PMMA surface and allow for a good attachment of GUVs to it an avidin-biotin link was utilized. The coupon was cleaned with ethanol and the well was washed with phosphate buffer solution (PBS) twice. Then, the well was filled with approximately 250 µl of biotinylated bovine serum albumin (Pierce™, Thermo Scientific) and incubated at room temperature for 1 hour. Then, the well was washed twice with PBS and filled with 250 µl of avidin solution and incubated for another 2 hours. Afterwards, the well was washed twice with PBS and the coupon was glued to the sonotrode using a cyanoacrylate glue (Loctite 422) and was ready to be filled with GUVs solution.

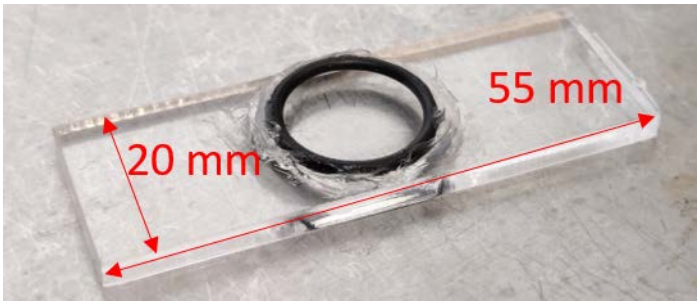

(a) Modified PMMA coupon with attached O-ring

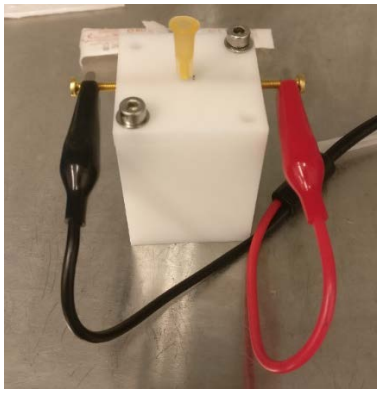

(b) Electroformation device for producing GUVs

Fig. 2 Device for testing and producing GUVs. (a) A modified PMMA coupon, (b) An electroformation chamber connected to a signal generator.

The GUVs were then prepared according to the electroformation protocol presented by Pereno *et al.* [11]. Two steel needles were covered with a lipid solution of DOPC and 1,2-dipalmitoyl-sn-glycero-3-phosphoethanolamine-N-(cap biotinyl) (sodium salt) (molar ratio of 10:1) dissolved in chloroform to the final concentration of 1 mg of lipids per 1 ml of chloroform. The needles were left to dry for 1 hour and then submerged in a custom electroformation chamber (**Fig. 2**(b)) filled with 3 ml of 200 mM/ml sucrose solution, with addition of blue food dye. A signal generator was then connected to the needles and the electroformation took place in two steps: in the first one, 10 Hz signal with 5 V (peak-to-peak) was applied for two hours, then the frequency was lowered to 5 Hz (also at 5 Vpp) for an additional half an hour. Afterwards, the GUVs-rich sucrose solution was transferred to a vial filled with PBS in a proportion of 1:1. Note, that to transfer the GUVs, the tip of the pipette was cut-off to increase the diameter of orifice and thus reduce the shear stress on GUVs. The solution was then gently mixed and small quantity (250 µl) was transferred into the well on the surface of PMMA. Due of the density difference between the sucrose solution and PBS the GUVs sink to the bottom of the well and form avidin-biotin link during incubation period of about 30 min. After the incubation period most of the liquid in the well was gently removed with a pipette, leaving only attached GUVs and a thin film on the surface.

The coupon containing attached GUVs was placed under an inverted microscope (Olympus IX71) that was customized to image the GUVs under ultrasonic deformation (**Fig. 3**). The Shimadzu HPV-X camera was connected to the camera port and a 50 × objective was used to record the movement of the GUVs at 500 kfps. Under such magnification one pixel corresponds to 0.64 µm, which was validated using a calibration grid with a pitch of 30 µm. Due to the combination of very high magnification and frame rate the lighting was particularly challenging. Here, we used a pulsed laser (Cavilux, Cavitar) that sends light pulses of up to 150 ns long synchronized with the camera acquisition rate. The coupon was then excited with the sonotrode at 30% of the maximal power of the sonotrode and the GUVs were imaged during the steady-state oscillation.

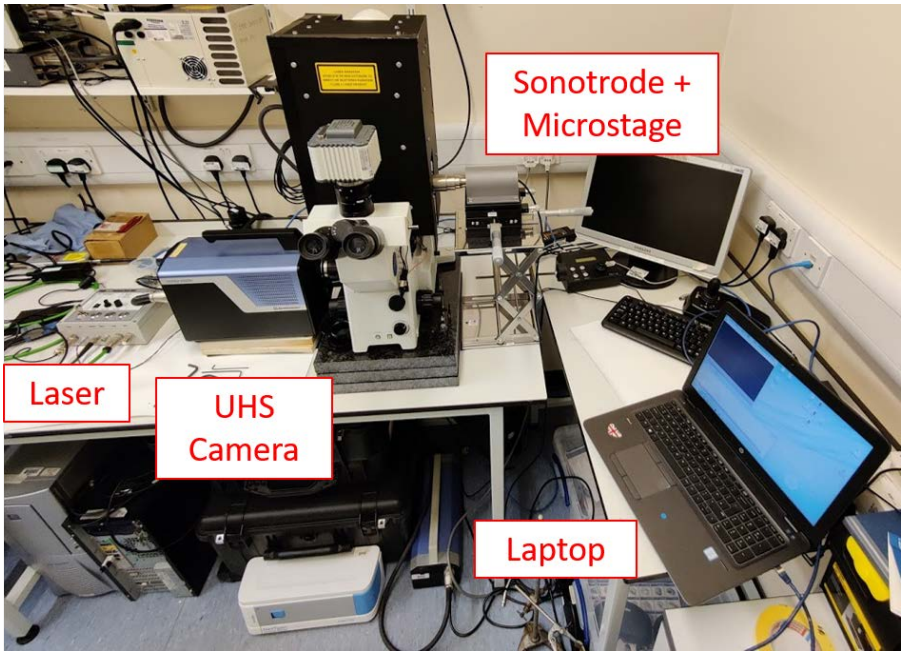

Fig. 3 The modified microscope for imaging GUVs using the ultra-high speed camera.

RESULTS

During the calibraiton step, the displacement fields were measured using the grid method, spatially smoothed using Gaussian filter with the window size of 35 pixels and temporarily (also using Gaussian filter) with the window size of 5 frames. The displacements were then differentiated spatially using central finite difference and resulting strains were averaged for each cross section and fitted with a sine function to measure frequency and amplitude of the excitation. It was found that the measured frequency (19.8 kHz) was matching the sonotrode's reference 20 kHz, with the small difference being explained by the frequency tracking system of the sonotrode to maximise the resonance. At the chosen level of excitation (30% of maximal power of the sonotrode) the longitudinal strain at the region corresponding to the O-ring ranges between 800 and 1000 µm/m (**Fig. 4**).

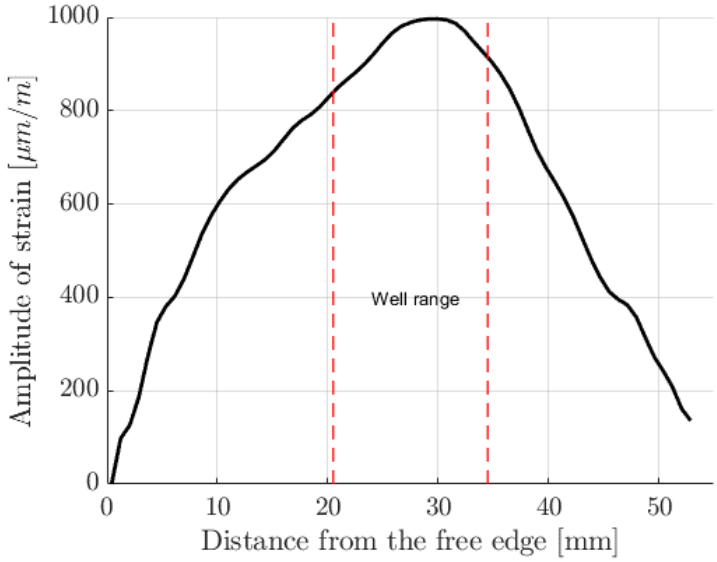

Fig. 4 Amplitude of average strain for each cross section along the length of the PMMA coupon.

A single GUV was isolated and imaged at 500 kfps (**Fig. 5**). A subpixel edge detection algorithm [12] was employed to track the movement of the vesicle and a circle was fitted at each frame to the processed data. The fitting allows to follow both the rigid body displacement (due to downstream effects, misorientation of the sonotrode with the camera frame, etc.) as well as the change in the radius which corresponds to deformation of the GUV. Due to relatively large magnitude of the rigid body movement (a few pixels) the signal-to-noise ratio was excellent, as shown in **Fig. 6**(a). Conversely, the detected change in radius of the GUV was much more subtle with the amplitude of (deviation from the mean) 0.009 pixel, which corresponds to the strain amplitude of 886 µm/m (**Fig. 6**(b)). In both cases the measured frequency was close to 20.0 kHz (20.0 kHz and 19.7 kHz for displacements and the radius respectively).

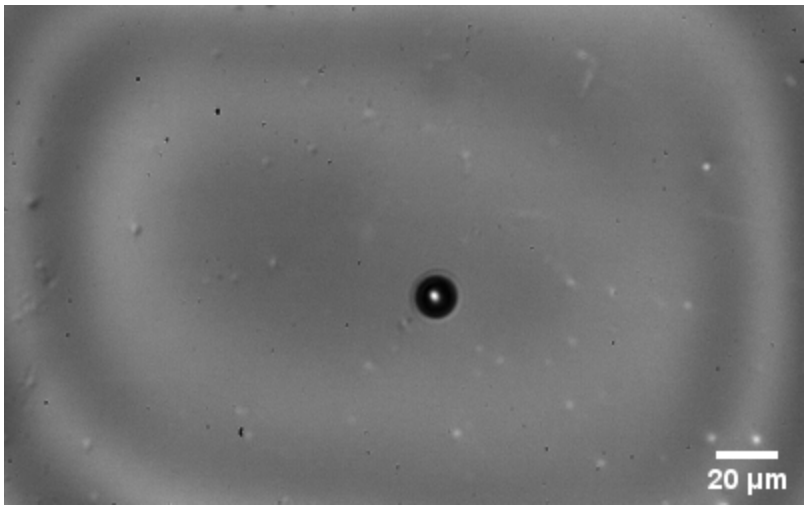

Fig. 5 An isolated GUV used to validate the test.

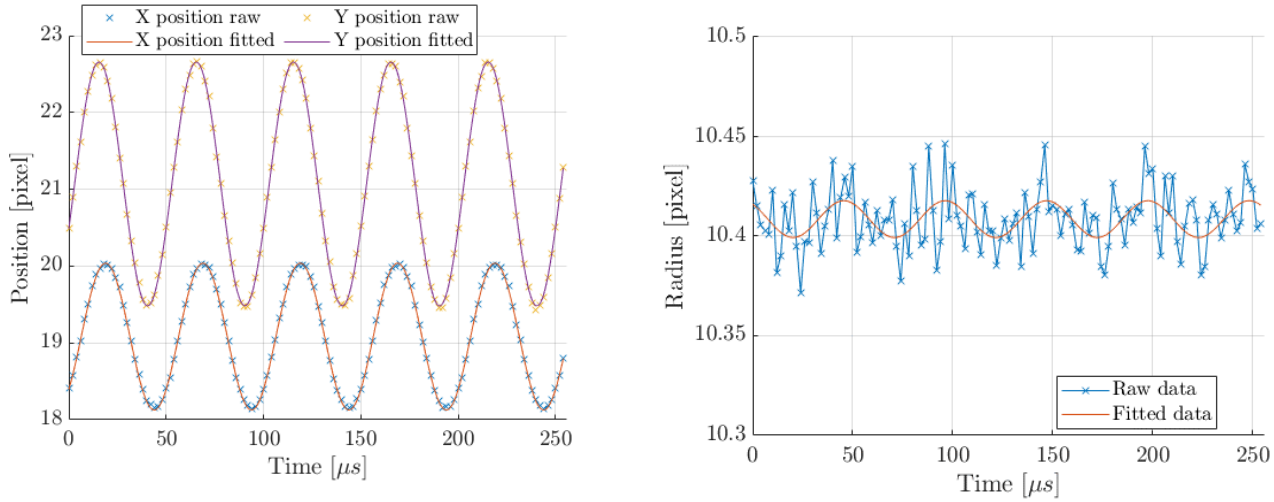

(a) Rigid body movement of the centre of the GUV

(b) Evolution of GUV's radius with time

Fig. 6 Analysis of the movement and deformation of the imaged GUV. (a) Displacement of the centre, (b) Evolution of radius (deformation).

DISCUSSION

The results indicate that the amplitude of the radius change is in good agreement with what was predicted using the macroscopic calibration protocol. This suggests that the proposed protocol can be used to controllably load attached entities by just controlling the amplitude of the sonotrode oscillation, leading to different level of deformation of the substrate (in the milistrain range). To increase the number of replicates, more wells can be placed on the surface of the substrate, each one being characterized by different amplitude of the strain (e.g. a well centered 10 mm away from the free edge would be expected to deform GUV up to 600 µm/m, see **Fig. 4**).

It is worth noting that analyzed GUV was very small (diameter of roughly 13 µm), thus the strain measurements were very noisy. It had also a very good contrast with the background, likely due to the blue food dye that absorbed the monochromatic (red) laser light. The contrast is critical for subpixel edge detection. In other cases (**Fig. 7**) the algorithm failed to detect the deformation. As the noise floor for the algorithm is constant (~0.01 px) it is possible to further improve the measurements by increasing the size of GUVs in terms of pixels. This can be done in two independent ways: by producing larger GUVs and

using higher magnification. The former can be achieved by placing larger volumes of the GUVs solution in the well (statistically there will be more large GUVs), as well as optimizing the electroformation protocol. The larger magnification can be achieved by either employing more powerful objectives, or by adding an optical element to the microscope (e.g. Olympus IX71 can add additional 1.6 × magnification to the current setup).

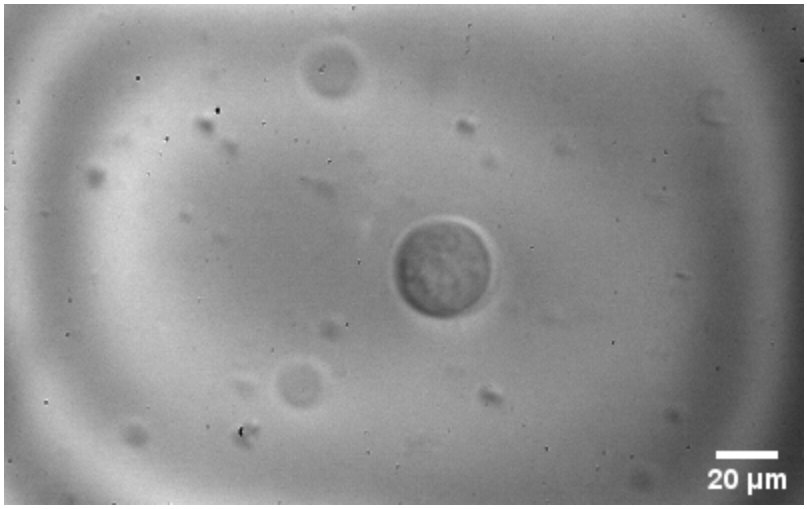

Fig. 7 A larger GUV imaged with the ultra-high speed camera with much poorer contrast.

Due to high number of cycles per second (20 kHz) the protocol is very promising for studying fatigue of cell membrane, as it would take only 15 minutes of continuous exposure to reach as much as 20 million cycles. One of practical challenges is the self-heating of the substrate due to viscous energy dissipation. A preliminary study was run by recording the temperature increase at the centre of the PMMA coupon using high speed infrared detector (Telops M2k), as shown in **Fig. 8**(a). The test protocol consisted of sonotrode turning on for 1s followed by resting period (sonotrode is off) of 10s. It was found that such pattern leads to a significant increase in the temperature of PMMA over a few cycles. By increasing the off portion to 60 s it was possible to stabilize the temperature in the middle between 32°C and 40°C (**Fig. 8**(b)). In future this could be improved on by either employing a small fan next to the experimental setup, or changing the PMMA substrate to a glass one.

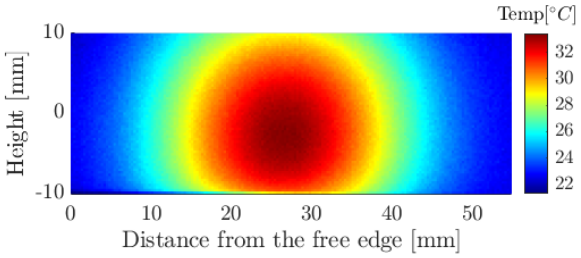

(a) Full-field map of the temperature field after steady state has been reached.

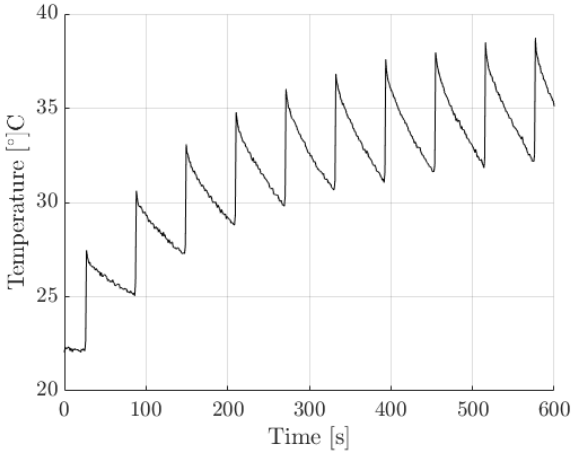

(c) Evolution of temperature in the middle of the coupon with the excitation 1s ON and 60s OFF.

Fig. 8 Full-field map of the temperature field. (a) Plot of the entire surface of the PMMA coupon, (b) History of a single point in the middle of the coupon.

CONCLUSION AND FUTURE WORK

The proposed protocol allows to cyclically load attached GUVs to a known deformation level at ultrasonic frequencies. After calibrating the sonotrode/substrate system externally using an ultra-high speed camera the protocol could be used to test the biological response of GUVs/cells regardless of access to such camera, as the deformation could be inferred from the calibration.

One of interesting applications of such test is to study fatigue of cell membrane modelled with GUVs. The advantage of such model is that it removes a lot of biological factors, such as repair of membrane, cell death etc. Simply by increasing the number of cycles at constant deformation the deterioration of the vesicles could be monitored i.e. in terms of increased diffusivity of the GUV. This could be studied by including a fluorophore in the sucrose solution in which the GUVs are formed. Initially only GUVs would produce fluorescent signal which intensity could be tracked and compared against the background as a function of number of oscillations.

Another interesting application would be to study apoptosis of cells under ultrasonic deformation. Cells could be grown either in wells or along the entire substrate, each group exposed to different thermo-mechanical history. By sweeping through different amplitudes and durations of pulses the relationship between the ultrasonic excitation and cell death could be established. This is a very promising prospect and will be pursed in the near future.

Finally, to get a better insight into deformation of GUVs (and cells in future), instead of using ultra-high speed camera to time-resolve the deformation one could employ a high resolution camera and use a stroboscopic technique (e.g. using the pulsed laser employed in this study) to reconstruct the deformation with much better spatial resolution by using the steady-steady assumption. Such assumption is well-grounded and the data presented in this contribution supports its validity. This could be particularly important when looking at the deformation of cells as their shape is irregular and couldn't be simply approximated by a change in radius. Instead, other image processing methods should be employed (e.g digital image correlation).

ACKNOWLEDGEMENTS

The authors gratefully acknowledge EPSRC for funding through grants EP/L026910/1 and EP/R045291/1.

REFERENCES

[1] A. K. Amin, J. S. Huntley, P. G. Bush, A. H. Simpson, and A. C. Hall, "Chondrocyte death in mechanically injured articular cartilage--the influence of extracellular calcium," *J Orthop Res*, vol. 27, no. 6, pp. 778-84, Jun 2009.

[2] M. Marrelli *et al.*, "Dental Pulp Stem Cell Mechanoresponsiveness: Effects of Mechanical Stimuli on Dental Pulp Stem Cell Behavior," *Front Physiol*, vol. 9, p. 1685, 2018.

[3] S. M. Uddin *et al.*, "Chondro-protective effects of low intensity pulsed ultrasound," *Osteoarthritis Cartilage*, vol. 24, no. 11, pp. 1989-1998, Nov 2016.

[4] S. Manaka *et al.*, "Low-intensity pulsed ultrasound-induced ATP increases bone formation via the P2X7 receptor in osteoblast-like MC3T3-E1 cells," *FEBS Lett*, vol. 589, no. 3, pp. 310-8, Jan 30 2015.

[5] N. Kudo, "High-Speed In Situ Observation System for Sonoporation of Cells With Size- and Position-Controlled Microbubbles," *IEEE Trans Ultrason Ferroelectr Freq Control*, vol. 64, no. 1, pp. 273-280, Jan 2017.

[6] F. Yuan, C. Yang, and P. Zhong, "Cell membrane deformation and bioeffects produced by tandem bubble-induced jetting flow," *Proc Natl Acad Sci U S A*, vol. 112, no. 51, pp. E7039-47, Dec 22 2015.

[7] Q. Gao, P. R. Cooper, A. D. Walmsley, and B. A. Scheven, "Role of Piezo Channels in Ultrasound-stimulated Dental Stem Cells," *J Endod*, vol. 43, no. 7, pp. 1130-1136, Jul 2017.

[8] Q. Gao, A. D. Walmsley, P. R. Cooper, and B. A. Scheven, "Ultrasound Stimulation of Different Dental Stem Cell Populations: Role of Mitogen-activated Protein Kinase Signaling," *J Endod*, vol. 42, no. 3, pp. 425-31, Mar 2016.

[9] R. Seghir and F. Pierron, "A Novel Image-based Ultrasonic Test to Map Material Mechanical Properties at High Strain-rates," *Experimental Mechanics*, vol. 58, no. 2, pp. 183-206, 2017.

[10] M. Grédiac, F. Sur, and B. Blaysat, "The Grid Method for In-plane Displacement and Strain Measurement: A Review and Analysis," *Strain*, vol. 52, no. 3, pp. 205-243, 2016.

[11] V. Pereno *et al.*, "Electroformation of Giant Unilamellar Vesicles on Stainless Steel Electrodes," *ACS Omega*, vol. 2, no. 3, pp. 994-1002, Mar 31 2017.

[12] A. Trujillo-Pino, K. Krissian, M. Alemán-Flores, and D. Santana-Cedrés, "Accurate subpixel edge location based on partial area effect," *Image and Vision Computing*, vol. 31, no. 1, pp. 72-90, 2013.